NEOPLASIA
www.neoplasia.com

Volume 19 Number 1 January 2017 pp. 1–7 1

SDF-1 Blockade Enhances Anti-VEGF Therapy of Glioblastoma and Can Be Monitored by MRI[1,2]

Lei Deng[*,3], Jason H. Stafford[*], Shie-Chau Liu[*,4], Sophia B. Chernikova[*,5], Milton Merchant[†], Lawrence Recht[†] and J. Martin Brown[*]

*Department of Radiation Oncology, Stanford University, A246, 1050A Arastradero Rd., Palo Alto, CA 94304-1334, USA; [†]Department of Neurology, Stanford University School of Medicine, 875 Blake Wilbur Dr., Stanford, CA 94305, USA

Abstract

Despite the approval of antiangiogenic therapy for glioblastoma multiforme (GBM) patients, survival benefits are still limited. One of the resistance mechanisms for antiangiogenic therapy is the induction of hypoxia and subsequent recruitment of macrophages by stromal-derived factor (SDF)-1α (CXCL-12). In this study, we tested whether olaptesed pegol (OLA-PEG, NOX-A12), a novel SDF-1α inhibitor, could reverse the recruitment of macrophages and potentiate the antitumor effect of anti–vascular endothelial growth factor (VEGF) therapy. We also tested whether magnetic resonance imaging (MRI) with ferumoxytol as a contrast agent could provide early information on macrophage blockade. Orthotopic human G12 glioblastomas in nude mice and rat C6 glioblastomas were employed as the animal models. These were treated with bevacizumab or B-20, both anti-VEGF antibodies. Rats were MR imaged with ferumoxytol for macrophage detection. Tumor hypoxia and SDF-1α expression were elevated by VEGF blockade. Adding OLA-PEG to bevacizumab or B-20 significantly prolonged the survival of rodents bearing intracranial GBM compared with anti-VEGF therapy alone. Intratumoral CD68+ tumor associated macrophages (TAMs) were increased by VEGF blockade, but the combination of OLA-PEG + VEGF blockade markedly lowered TAM levels compared with VEGF blockade alone. MRI with ferumoxytol as a contrast agent noninvasively demonstrated macrophage reduction in OLA-PEG + anti-VEGF–treated rats compared with VEGF blockade alone. In conclusion, inhibition of SDF-1 with OLA-PEG inhibited the recruitment of TAMs by VEGF blockage and potentiated its antitumor efficacy in GBM. Noninvasive MRI with ferumoxytol as a contrast agent provides early information on the effect of OLA-PEG in reducing TAMs.

Neoplasia (2017) 19, 1–7

Introduction

Despite the recent approval of bevacizumab for treatment of glioblastoma (GBM), the survival of such patients is still poor. GBMs treated with bevacizumab invariably progress, and first-line use of bevacizumab did not improve overall survival in two randomized trials [1,2]. Thus, therapies overcoming resistance or evasion of VEGF blockade are urgently needed [3].

Bevacizumab, an antibody blocking vascular endothelial growth factor (VEGF), exerts its function by inhibiting tumor angiogenesis [4]. Studies have shown that antiangiogenic therapy can induce tumor hypoxia and lead to an influx of bone marrow–derived cells, including macrophages, into the tumors and facilitate therapeutic resistance [5,6]. Tumor-associated macrophages (TAMs) are known to promote tumor growth by their proangiogenic action [7–9].

We have previously demonstrated that hypoxia is responsible for macrophage infiltration of tumors postirradiation by upregulating

Abbreviations: GBM, glioblastoma multiforme; OLA-PEG, olaptesed pegol; TAMs, tumor-associated macrophages; VEGF, vascular endothelial growth factor.

Address all correspondence to: J. Martin Brown, PhD, Dept Neurology, 1201 Welch Road, MSLS P256, Stanford, CA 94305.
E-mail: mbrown@stanford.edu

[1] The work was supported by grants from the National Institutes of Health (grant number R01 CA149318). L. D. was supported by China Scholarship Council.
[2] Conflict of Interest: none.

[3] Present address: Department of Thoracic Oncology, Cancer Center, West China Hospital/School of Medicine, Sichuan University, 37, Guoxue Lane, Chengdu, Sichuan, 610,041, China.
[4] Present address: Radiological Sciences Laboratory, Department of Radiology, Stanford University School of Medicine, 1201 Welch Rd., Lucas Center for Medical Imaging, Stanford, CA 94305, USA.
[5] Present address: Departments of Neurology and Neurosurgery 1201 Welch Road, P151 and P254 Stanford, CA 94305.

Received 16 November 2014; Revised 8 November 2016; Accepted 15 November 2016

1476-5586
http://dx.doi.org/10.1016/j.neo.2016.11.010

stromal cell–derived factor 1-α (SDF-1α) (CXCL-12) and that tumor response can be enhanced by blocking the SDF-1 pathway [10]. Olaptesed pegol (OLA-PEG, previously known as NOX-A12) is a novel PEGylated mirror-image RNA oligonucleotide with high binding affinity to SDF-1. We previously showed the inhibitory effect of OLA-PEG on SDF-1α–dependent migration of monocyte *in vitro* and the prolonged survival of rats with autochthonous brain tumors treated with the drug combined with irradiation [11]. Because tumor irradiation blocks or severely limits local angiogenesis [12], we asked the question using two GBM models of whether blocking the SDF-1 pathway would increase the therapeutic efficacy of anti-VEGF therapy, which also targets angiogenesis,

Ferumoxytol, a product containing ultrasmall superparamagnetic iron oxide nanoparticles, is an FDA-approved iron supplement for anemic patients. As it can be phagocytosed by TAMs and imaged by magnetic resonance (MR) [13,14], we also investigated whether it could be used to noninvasively image by MR imaging (MRI) changes in TAM levels in tumors produced by anti-VEGF therapy combined with SDF-1 blockage.

In the present study, we found that SDF-1 blockade could potentiate the therapeutic effect of anti-VEGF therapy in GBM animal models by inhibiting macrophage recruitment and further reduces tumor vasculature. To provide a clinically relevant early therapeutic evaluation, we also found that reduction in macrophage influx by OLA-PEG could be noninvasively imaged by MRI with ferumoxytol as a contrast agent.

Materials and Methods

Tumors and Animals

GBM12 (G12), a serially passaged human glioblastoma, was a generous gift from Dr. Jann Sarkaria (Mayo Clinic, MN) and was passaged as previously described [15]. A total of 300,000 G12 cells were implanted intracranially into nude mice (NCI Frederick, MD). Rat C6 cells were obtained from ATCC and were authenticated by them. A total of 500,000 cells were injected intracranially into Sprague-Dawley rats purchased from Charles River. Tumor cells were injected into the brain as previously described [10]. All animal procedures were approved by Stanford University's Administrative Panel on Laboratory Animal Care. For survival analysis, animal numbers are as follows: for G12 (bevacizumab) experiment: G12 control (n = 5), OLA-PEG (n = 5), Beva (n = 6), Beva + OLA-PEG (n = 6); for C6 (B-20) experiment: C6 control (n = 8), treated with OLA-PEG (n = 10), B-20 (n = 14), or B-20 + OLA-PEG (n = 14)

Drug Treatment

Because of the different tumor models and different anti-VEGF antibodies, treatment regimens differed in dose and time points in the two models. OLA-PEG (a generous gift from NOXXON Pharma AG, Germany) was prepared as previously described [11], and the solution was injected subcutaneously every other day at a dose of 10 mg/kg until animal sacrifice. Bevacizumab (Genentech, CA) was injected intraperitoneally at a dose of 5 mg/kg, twice a week, based on a previous report [16]. B-20 (Genentech, CA) was given once, at a dose of 5 mg/kg. B-20 is a cross-species VEGF-blocking antibody [17,18]. For mice with G12 tumors, treatment was started 14 days after cell implantation; for rats with C6 tumors, OLA-PEG was started 6 days and B-20 7 days after implantation. Necrotic tumors were not harvested when collecting samples.

MRI Assessment of Intracerebral Macrophage Influx

MRI of C6 tumors was performed 7 days after treatment initiation with a 1-T animal MR scanner (Bruker ICON) located in the Stanford Small Animal Imaging Center. MRI scans were taken prior to and 24 hours after intravenous injection of 27.92 mg/kg (0.5 mmol [Fe]/kg) ferumoxytol. Ferumoxytol was a generous gift from Dr. Heike E. Daldrup-Link (Stanford University, CA).

Coronal T2-weighted RARE pulse sequences were obtained with a 180° flip angle, a 3300-millisecond repetition time (TR), and a 120-millisecond echo time (TE). T1 relaxation time was obtained with a T1-FLASH-T1mapIR sequence with a 218.7-millisecond TR, a 6.0-millisecond TE, and multiple increasing inversion time (TI) of 25 to 200 milliseconds. T2 relaxation time was obtained with T2map-MSME sequence with a 1500-millisecond TR and multiple echo of 17 to 119 milliseconds. T2* relaxation time was obtained with Flash-bas sequence with 325.7-millisecond TR, an increasing echo of 9 to 54 milliseconds, and a 30° flip angle. All sequences (2-10 acquisitions) were acquired with a field of view of 27 × 27 mm, a matrix of 160 × 160 pixels, and a slice thickness of 1.0 mm.

The acquired MR images were transferred as DICOM images and processed by the ParaVision 5 software. Average signal intensities of the whole tumor, tumor rim, and tumor center as well as background noise were measured by operator-defined regions of interest. T2-relaxation times of the tumor were calculated based on T2map-MSME sequences and converted to R2-relaxation rates (R2. 1/T2), which is proportional to contrast agent concentration. The relative change in R2 (ΔR2) between pre- and postcontrast MRI was determined as a quantitative measure of tumor contrast enhancement. In addition, T1 and T2* relaxation rates of the tumors were calculated from the multi-TI and multiecho pulse sequences using nonlinear function least square curve fitting on a pixel-by-pixel basis. T_1 relaxation times were calculated using inversion recovery sequences with a fixed TR of 218.7 milliseconds, a TE of 6.0 milliseconds, and increasing TI of 25 to 200 milliseconds. T_2^* relaxation times were calculated with a fixed TR of 325.7 milliseconds and increasing TEs of 9 to 54 milliseconds. The relaxation times of the tumors were derived by region of interest measurements of the tumors on the resultant T1, T2, and T2* maps, and the results were converted to R1, R2, and R2* relaxation rates (s − 1).

Immunofluorescent Staining and Quantification

Endothelial cells were stained by rat anti-mouse CD31 for G12 tumors at a 1:200 dilution (BD Biosciences). Macrophages were stained with a dilution of 1:400 rabbit anti-mouse/rat CD68 (Abcam). SDF-1α antibody (Santa Cruz Biotechnology) was used at a concentration of 1:100. Tumor hypoxia was evaluated by staining with rabbit anti-human hypoxia inducible factor (HIF)-1α (Abcam, 1:100 dilution). Frozen sections were stained with primary antibodies overnight in a cold room, and Alexa Fluor 488 anti-rat or Alexa Fluor 555 anti-rabbit antibodies were used for secondary antibodies where appropriate (Life Technologies, 1:500 dilution) for 1 hour at room temperature. Immunofluorescent images were acquired as previously described [10]. Only intratumoral area images were acquired by identifying the nuclei density difference. Signal pixels were measured by Image-Pro Plus (MediaCybernetics) using a ×20 objective with ×10 eyepieces of the fluorescence microscope.

Statistical Analysis

Statistical analysis was performed as previously described [10]. Student's t test was used when appropriate. $P < .05$ was considered

statistically significant. Prism (GraphPad) was used for statistical calculations. Survival analysis was calculated using the Gehan-Breslow-Wilcoxon (GBW) test. The GBW test puts more emphasis on early death events difference, which is the case in our animal model with control animals all dying within a very short time period [19].

Results

Anti-VEGF Treatment Increases Tumor SDF-1α Levels

We previously showed that radiation treatment of experimental GBM tumors increased tumor hypoxia as well as HIF-1α and SDF-1α levels, thereby mobilizing macrophages to the tumors [10]. Increased tumor hypoxia has been suggested to be one of the mechanisms of resistance to antiangiogenic treatment by increasing SDF-1α levels [20]. Compared with untreated control animals, immunofluorescent staining demonstrated that B-20 significantly increased the expression of SDF-1α in C6 tumors 7 days after B-20 treatment (Figure 1, *A* and *B*). Similarly, SDF-1α and HIF-1α were significantly higher in bevacizumab-treated G12 tumors compared with untreated controls (Figure 1, *C–F*), consistent with other reports [21].

Macrophage Infiltration by Anti-VEGF Treatment Can Be Blockaded by OLA-PEG and Imaged by MR

Because we previously showed that SDF-1α mobilized macrophages into irradiated tumors [10], we asked if this is also the case for anti-VEGF–treated tumors. Similar to our irradiation results, B-20–treated C6 tumors had significantly increased CD68+ macrophages 7 days after treatment (Figure 2, *A* and *B*). Adding OLA-PEG, an SDF-1α inhibitor, to B-20 significantly decreased the macrophage influx as expected. To provide a more clinically relevant and early imaging of the effect of SDF-1 blockade by OLA-PEG, we utilized ferumoxytol, an FDA-approved iron supplement, for MR imaging in the rat C6 glioblastoma model. Ferumoxytol has been shown to be preferentially phagocytized by TAMs but not by cancer cells [13]. ΔR2, which is a measure of changes in iron concentration, decreased progressively over 24 hours after intravenous tail vein injection of ferumoxytol (Supplemental Figure S1). We therefore MR imaged C6-bearing rat brain at pre- and 24-hour postinjection 7 days after treatment initiation. The combination of OLA-PEG and B20 antibody showed less MR contrast, demonstrated by significantly less ΔR2 enhancement compared with B20 alone (Figure 2, *C* and *D*).

OLA-PEG Decreases CD68+ Macrophage Infiltration by Bevacizumab and Further Reduces Microvessel Density in G12 GBM Tumor

We also tested the macrophage infiltration in human G12 models treated with bevacizumab. Compared with control mice, bevacizumab significantly increased CD68+ macrophages in tumors (Figure 3, *A* and *B*). However, OLA-PEG + bevacizumab–treated tumors had considerably fewer CD68+ TAMs compared with bevacizumab alone, highlighting the effect of OLA-PEG. Because we had previously shown that macrophages mobilized by SDF-1α facilitated tumor recurrence after irradiation by promoting vasculature regrowth [10], we asked whether OLA-PEG could further decrease microvessel density compared with anti-VEGF therapy alone.

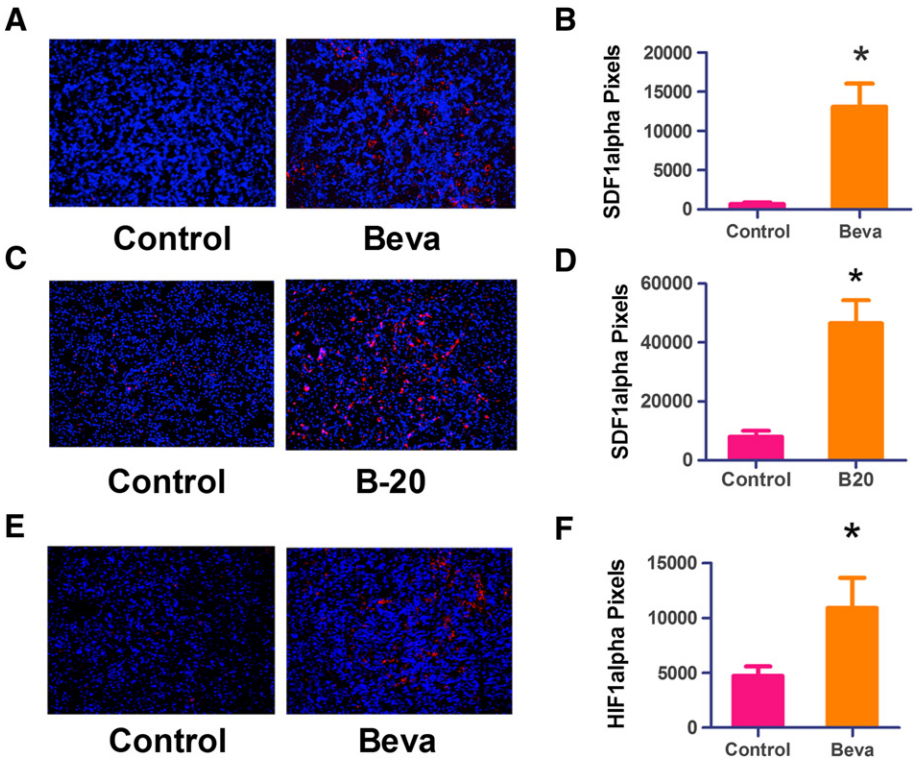

Figure 1. Anti-VEGF antibody increased SDF-1α and HIF-1α levels in GBM. (A) Representative images (×20) of SDF-1α expression in control and B-20–treated C6 tumors. Red: SDF-1α; blue: DAPI. (B) Quantification of A ($n = 3$ for each group). B-20 significantly increased SDF-1α expression (*, Student's t test, $P < .05$). (C) Representative images (×20) of SDF-1α expression in control and bevacizumab-treated G12 tumors. Red: SDF-1α; blue: DAPI. (D) Quantification of C ($n = 3$ for each group). Bevacizumab significantly increased SDF-1α expression (*, Student's t test, $P < .0001$). (E) Representative images (×20) of HIF-1α expression in control and bevacizumab-treated G12 tumors. Red: HIF-1α; blue: DAPI. (F) Quantification of E ($n = 3$ for each group). Bevacizumab significantly increased HIF-1α expression (*, Student's t test, $P < .05$).

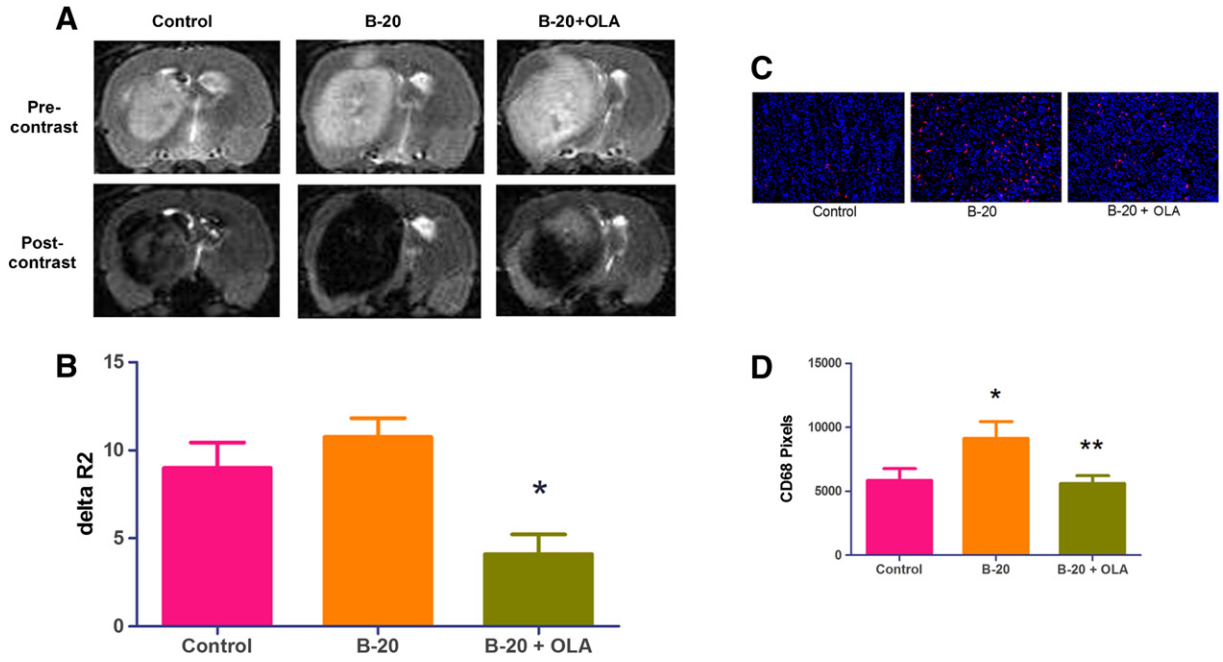

Figure 2. OLA-PEG decreased macrophage influx by B-20 and can be imaged by ferumoxytol-contrasted magnetic resonance. (A) Representative images (×20) of CD68+ macrophage staining in frozen C6 tumor sections 7 days after starting B-20. Red: CD68; blue: DAPI. (B) Quantification of A ($n = 3$ for each group). B-20 significantly recruited macrophages compared with control (*, Student's t test, $P < .05$), and OLA-PEG (OLA) + B-20 group had fewer macrophages compared with B-20 alone (**, Student's t test, $P < .05$). (C) Representative images of MRI. Precontrast image was obtained 7 days after treatment initiation with a 1-T MR scanner. A total of 27.92 mg/kg ferumoxytol was intravenously injected after precontrast scan. Postcontrast scan was performed 24 hours after ferumoxytol injection. (D) ΔR2 quantification of C ($n = 5$ for each group). OLA-PEG (OLA) + B-20 treatment had significantly smaller ΔR2 value compared with B-20 group (*, Student's t test, $P < .01$).

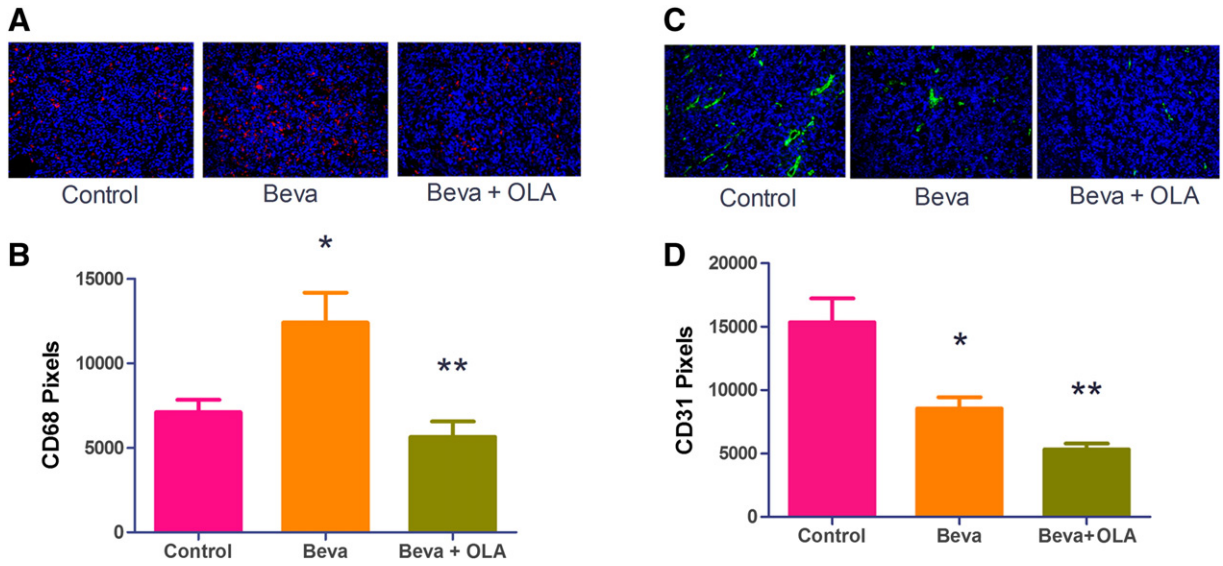

Figure 3. OLA-PEG (OLA) decreased CD68+ TAMs by bevacizumab (Beva) and microvessel density in G12 tumors. (A) Representative images (×20) of CD68+ macrophage staining in frozen G12 tumor sections. Red: CD68; blue: DAPI. All areas in the image were intratumoral. (B) Quantification of A ($n = 3$ for each group). Bevacizumab increased macrophages in G12 tumors compared with control tumor (*, Student's t test, $P < .05$); OLA-PEG (OLA) + Beva–treated mice had fewer TAMs compared with the Beva-alone group (**, Student's t test, $P < .01$). (C) Representative images (×20) of CD31+ vessel staining in G12 tumor sections. Green: CD31; blue: DAPI. All areas in the image were intratumoral. (D) Quantification of C ($n = 3$ for each group). Beva decreased CD31+ vessel density compared with controls (*, Student's t test, $P < .05$), and OLA + Beva had still fewer vessels per field (**, Student's t test, $P < .01$ compared with Beva alone).

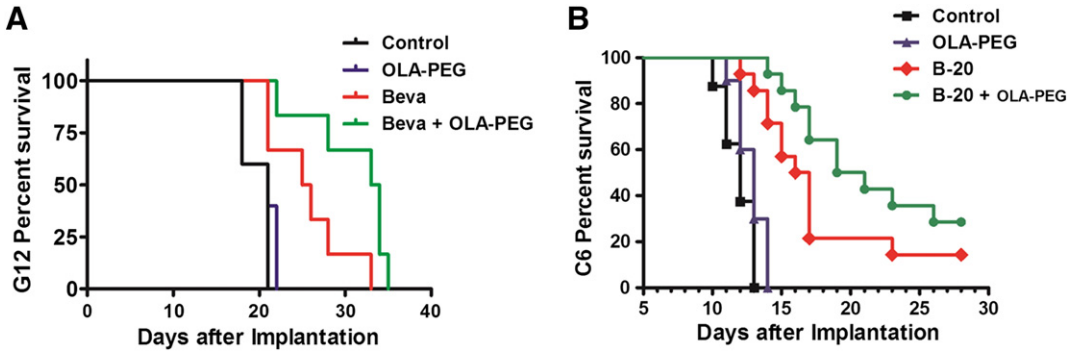

Figure 4. OLA-PEG prolonged survival of Beva or B-20–treated rodents. OLA-PEG was given subcutaneously every other day at a dose of 10 mg/kg until animal sacrifice or death. (A) Nude mice implanted intracranially with G12 tumors were treated starting 14 days after implantation with control (n = 5), OLA-PEG (n = 5), Beva (n = 6), or Beva + OLA-PEG (n = 6). Bevacizumab was given intraperitoneally at a dose of 5 mg/kg two times weekly. (B) Rats with intracranially implanted C6 GBM cells were untreated (n = 8) or treated with OLA-PEG (n = 10), B-20 (n = 14), or B-20 + OLA-PEG (n = 14). OLA-PEG was started 6 days after implantation, and B-20 was given intraperitoneally one time on day 7 after implantation at a dose of 5 mg/kg.

Immunofluorescent staining showed fewer vessels in OLA-PEG and anti-VEGF combined treatment than anti-VEGF alone in G12 tumors (Figure 3, *C* and *D*), suggesting that the therapeutic benefit of adding OLA-PEG to bevacizumab is the result of robust decrease of tumor microvessel density.

OLA-PEG Prolongs Survival of Anti-VEGF–Treated Tumor-Bearing Rodents

We finally asked whether macrophage inhibition by adding OLA-PEG to anti-VEGF treatment produced survival benefits. Although OLA-PEG alone had no effect on the survival of tumor-bearing mice in the orthotopic G12 human glioblastoma model, nude mice receiving combined OLA-PEG and bevacizumab treatment had significantly longer survival than those treated with bevacizumab alone and control mice (Figure 4*A*). In contrast, untreated control and OLA-PEG only–treated mice had the same median survival of only 21 days. The median survival was extended from 25.5 days (Beva) to 33.5 days (Beva + OLA-PEG) (GBW P = .048). The survival benefit of OLA-PEG + bevacizumab compared with control (12.5 days) is more than triple that of bevacizumab alone compared with control (4 days). Similarly, OLA-PEG alone was not effective in C6 tumors, but adding OLA-PEG to B-20 prolonged survival from 16.5 (B-20 alone) days to 20 days (GBW P = .044) (Figure 4*B*). The untreated control rats lived with a median survival of 12.5 days, so OLA-PEG + B-20 combination almost doubled the survival benefit to control rat (7.5 days) compared with B-20 alone (4 days).

Discussion

GBM remains one of the most malignant human tumors, and treatment options are still limited for patients. Although bevacizumab has been approved for recurrent GBM and provides symptomatic relief, tumor progression follows and no overall survival benefit has been demonstrated [3]. We here show that macrophage influx by anti-VEGF antibody treatment can be effectively reduced by adding OLA-PEG, a novel SDF-1α inhibitor, to anti-VEGF treatment and further prolonged animal survival. The ferumoxytol-contrasted MRI signal reduction after adding OLA-PEG to bevacizumab also shows the potential for early clinical evaluation of the therapeutic effect.

Tumor-associated macrophages are proangiogenic [6,22]. Several authors have reported macrophage infiltration after treatment with vascular disruption or antiangiogenic agents and have shown that blocking this infiltration can potentiate treatment efficacy in preclinical models of other cancers [7,23–26]. Increased TAMs have been found in recurrent GBM patients after bevacizumab treatment and are associated with poor survival [27]. The SDF-1α-CXCR4 pathway has been shown to be important in mediating this infiltration [23,28,29], and elevated SDF-1α was found in rectal cancer patients after bevacizumab treatment [21]. Consistent with these reports, we found elevated SDF-1α in our animal models of GBM after anti-VEGF treatment, likely due to increased hypoxia and HIF-1α, as we have found in the irradiation setting [10,29]. We hereby summarize how OLA-PEG enhances the effect of anti-VEGF in Figure 5. Although AMD3100 is currently under clinical investigation in combination with bevacizumab for GBM patients (NCT01339039), it only blocks the interaction of SDF-1α with CXCR4. It has been reported that CXCR7 is also a receptor of SDF-1α and is highly expressed on tumor-associated endothelial cells [30]. Administration of an SDF-1α inhibitor both can block binding and can potentially provide further benefits.

Although some studies have shown direct tumor killing by blocking CXCR4 [30], we did not show survival benefits when using OLA-PEG alone. This finding, consistent with our previous report [11], indicates that at least the regimen of OLA-PEG we used did not extend survival by direct cell killing, of which the dose in this study is equivalent to the one used in human clinical trials. Instead, we found macrophage reduction when OLA-PEG was added to anti-VEGF therapy and a further decrease in microvessel density, supporting our hypothesis that OLA-PEG potentiates anti-VEGF treatment by inhibiting macrophage recruitment and thereby inhibiting tumor vasculature. When VEGF is blocked, tumor vasculature growth can be supported by a repertoire of proangiogenic factors secreted by macrophages [5], which are not critically needed when VEGF is abundant. This may explain why OLA-PEG alone did not improve animal survival in our study. We were also able to show elevated HIF-1α and SDF-1α expression after bevacizumab treatment, consistent with our previous and other's reports that HIF-1α is an important mediator of SDF-1α [10,23,31,32].

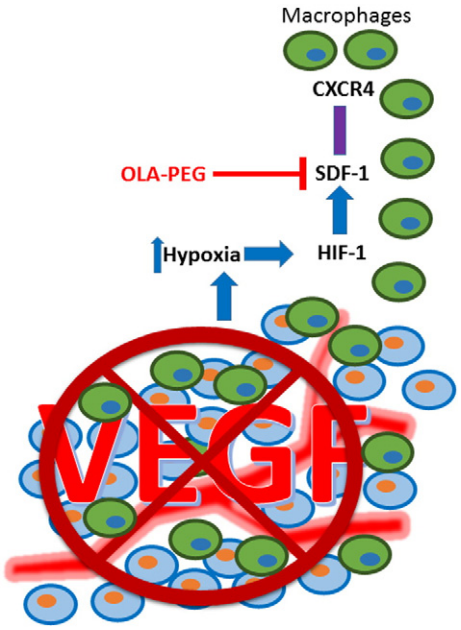

Figure 5. Model showing that how OLA-PEG enhances the effect of VEGF blockade by blocking macrophage infiltration.VEGF blockade increases tumor hypoxia and thereby upregulates HIF-1α, which results in the overexpression of SDF-1 in the tumor. SDF-1α interacts with CXCR4 expressed on macrophages and mobilizes them into the tumor, which can be inhibited by OLA-PEG.

Early clinical evaluation of therapeutic effect can be beneficial in order to monitor the treatment strategy and enable appropriate early modifications. Based on the mechanism of OLA-PEG, we used MRI of ferumoxytol as a contrast agent to noninvasively assess the macrophage reduction in the rat GBM. We found that the macrophage decrease was effectively demonstrated by MRI, consistent with our histological data. We also found that, within 4 days, the ferumoxytol signal decayed to below 20% of the maximum on day 1, which may allow repeated macrophage monitoring in the future. This suggests future clinical application of early therapeutic benefit evaluation in this approach as ferumoxytol has been approved by the FDA as a safe iron supplement for anemic patients [33]. Furthermore, compared with histological examination, MRI is noninvasive and provides information on the whole tumor.

Conclusions

Based on these preclinical data, we believe that the combination of OLA-PEG and bevacizumab warrants further evaluation by clinical trials. The adoption of MRI with ferumoxytol may be a promising method to evaluate the early clinical efficacy of strategies to reduce macrophage infiltration.

Supplementary data to this article can be found online at http://dx.doi.org/10.1016/j.neo.2016.11.010.

Acknowledgements

We would like to thank NOXXON Pharma A.G. for supplying OLA-PEG and Dr. Heike E. Daldrup-Link for supplying ferumoxytol and Dr. Jann Sarkaria for providing the human G12 tumor. The work was supported by grants from the National Institutes of Health (grant number R01 CA149318). L. D. was supported by China Scholarship Council.

References

[1] Gilbert MR, Dignam JJ, Armstrong TS, Wefel JS, Blumenthal DT, Vogelbaum MA, Colman H, Chakravarti A, Pugh S, and Won M, et al (2014). A randomized trial of bevacizumab for newly diagnosed glioblastoma. *N Engl J Med* **370**, 699–708.

[2] Chinot OL, Wick W, Mason W, Henriksson R, Saran F, Nishikawa R, Carpentier AF, Hoang-Xuan K, Kavan P, and Cernea D, et al (2014). Bevacizumab plus radiotherapy-temozolomide for newly diagnosed glioblastoma. *N Engl J Med* **370**, 709–722.

[3] Omuro A and DeAngelis LM (2013). Glioblastoma and other malignant gliomas: a clinical review. *JAMA* **310**, 1842–1850.

[4] Ferrara N, Hillan KJ, Gerber HP, and Novotny W (2004). Discovery and development of bevacizumab, an anti-VEGF antibody for treating cancer. *Nat Rev Drug Discov* **3**, 391–400.

[5] Ferrara N (2010). Role of myeloid cells in vascular endothelial growth factor-independent tumor angiogenesis. *Curr Opin Hematol* **17**, 219–224.

[6] De Palma M and Lewis CE (2013). Macrophage regulation of tumor responses to anticancer therapies. *Cancer Cell* **23**, 277–286.

[7] Bergers G and Hanahan D (2008). Modes of resistance to anti-angiogenic therapy. *Nat Rev Cancer* **8**, 592–603.

[8] Franklin RA, Liao W, Sarkar A, Kim MV, Bivona MR, Liu K, Pamer EG, and Li MO (2014). The cellular and molecular origin of tumor-associated macrophages. *Science* **344**, 921–925.

[9] Qian BZ and Pollard JW (2010). Macrophage diversity enhances tumor progression and metastasis. *Cell* **141**, 39–51.

[10] Kioi M, Vogel H, Schultz G, Hoffman RM, Harsh GR, and Brown JM (2010). Inhibition of vasculogenesis, but not angiogenesis, prevents the recurrence of glioblastoma after irradiation in mice. *J Clin Invest* **120**, 694–705.

[11] Liu SC, Alomran R, Chernikova SB, Lartey F, Stafford J, Jang T, Merchant M, Zboralski D, Zollner S, and Kruschinski A, et al (2014). Blockade of SDF-1 after irradiation inhibits tumor recurrences of autochthonous brain tumors in rats. *Neuro Oncol* **16**, 21–28.

[12] Ahn GO and Brown JM (2008). Matrix metalloproteinase-9 is required for tumor vasculogenesis but not for angiogenesis: role of bone marrow–derived myelomonocytic cells. *Cancer Cell* **13**, 193–205.

[13] Daldrup-Link HE, Golovko D, Ruffell B, Denardo DG, Castaneda R, Ansari C, Rao J, Tikhomirov GA, Wendland MF, and Corot C, et al (2011). MRI of tumor-associated macrophages with clinically applicable iron oxide nanoparticles. *Clin Cancer Res* **17**, 5695–5704.

[14] Yang R, Sarkar S, Korchinski DJ, Wu Y, Yong VW, and Dunn JF (2016). MRI monitoring of monocytes to detect immune stimulating treatment response in brain tumor. *Neuro Oncol*, [Published online: August 29, 2016].

[15] Carlson BL, Pokorny JL, Schroeder MA, and Sarkaria JN (2011). Establishment, maintenance and in vitro and in vivo applications of primary human glioblastoma multiforme (GBM) xenograft models for translational biology studies and drug discovery. *Curr Protoc Pharmacol* [Chapter 14, Unit 14 16].

[16] Huveldt D, Lewis-Tuffin LJ, Carlson BL, Schroeder MA, Rodriguez F, Giannini C, Galanis E, Sarkaria JN, and Anastasiadis PZ (2013). Targeting Src family kinases inhibits bevacizumab-induced glioma cell invasion. *PLoS One* **8**, e56505.

[17] Liang WC, Wu X, Peale FV, Lee CV, Meng YG, Gutierrez J, Fu L, Malik AK, Gerber HP, and Ferrara N, et al (2006). Cross-species vascular endothelial growth factor (VEGF)–blocking antibodies completely inhibit the growth of human tumor xenografts and measure the contribution of stromal VEGF. *J Biol Chem* **281**, 951–961.

[18] Raina S, Honer M, Kramer SD, Liu Y, Wang X, Segerer S, Wuthrich RP, and Serra AL (2011). Anti-VEGF antibody treatment accelerates polycystic kidney disease. *Am J Physiol Renal Physiol* **301**, F773–F783.

[19] Martinez RLMC and Naranjo JD (2010). A pretest for choosing between logrank and wilcoxon tests in the two-sample problem. *Metron* **LXVIII**, 111–125.

[20] Achyut BR, Shankar A, Iskander AS, Ara R, Angara K, Zeng P, Knight RA, Scicli AG, and Arbab AS (2015). Bone marrow derived myeloid cells orchestrate antiangiogenic resistance in glioblastoma through coordinated molecular networks. *Cancer Lett* **369**, 416–426.

[21] Xu L, Duda DG, di Tomaso E, Ancukiewicz M, Chung DC, Lauwers GY, Samuel R, Shellito P, Czito BG, and Lin PC, et al (2009). Direct evidence that bevacizumab, an anti-VEGF antibody, up-regulates SDF1alpha, CXCR4, CXCL6, and neuropilin 1 in tumors from patients with rectal cancer. *Cancer Res* **69**, 7905–7910.

[22] Galdiero MR, Bonavita E, Barajon I, Garlanda C, Mantovani A, and Jaillon S (2013). Tumor associated macrophages and neutrophils in cancer. *Immunobiology* **218**, 1402–1410.

[23] Welford AF, Biziato D, Coffelt SB, Nucera S, Fisher M, Pucci F, Di Serio C, Naldini L, De Palma M, and Tozer GM, et al (2011). TIE2-expressing macrophages limit the therapeutic efficacy of the vascular-disrupting agent combretastatin A4 phosphate in mice. *J Clin Invest* **121**, 1969–1973.

[24] Daly C, Eichten A, Castanaro C, Pasnikowski E, Adler A, Lalani AS, Papadopoulos N, Kyle AH, Minchinton AI, and Yancopoulos GD, et al (2013). Angiopoietin-2 functions as a Tie2 agonist in tumor models, where it limits the effects of VEGF inhibition. *Cancer Res* **73**, 108–118.

[25] Zhang W, Zhu XD, Sun HC, Xiong YQ, Zhuang PY, Xu HX, Kong LQ, Wang L, Wu WZ, and Tang ZY (2010). Depletion of tumor-associated macrophages enhances the effect of sorafenib in metastatic liver cancer models by antimetastatic and antiangiogenic effects. *Clin Cancer Res* **16**, 3420–3430.

[26] Hughes R, Qian BZ, Rowan C, Muthana M, Keklikoglou I, Olson OC, Tazzyman S, Danson S, Addison C, and Clemons M, et al (2015). Perivascular M2 macrophages stimulate tumor relapse after chemotherapy. *Cancer Res* **75**, 3479–3491.

[27] Lu-Emerson C, Snuderl M, Kirkpatrick ND, Goveia J, Davidson C, Huang Y, Riedemann L, Taylor J, Ivy P, and Duda DG, et al (2013). Increase in tumor-associated macrophages after antiangiogenic therapy is associated with poor survival among patients with recurrent glioblastoma. *Neuro Oncol* **15**, 1079–1087.

[28] Karin N (2010). The multiple faces of CXCL12 (SDF-1alpha) in the regulation of immunity during health and disease. *J Leukoc Biol* **88**, 463–473.

[29] Du R, Lu KV, Petritsch C, Liu P, Ganss R, Passegue E, Song H, Vandenberg S, Johnson RS, and Werb Z, et al (2008). HIF1alpha induces the recruitment of bone marrow–derived vascular modulatory cells to regulate tumor angiogenesis and invasion. *Cancer Cell* **13**, 206–220.

[30] Miao Z, Luker KE, Summers BC, Berahovich R, Bhojani MS, Rehemtulla A, Kleer CG, Essner JJ, Nasevicius A, and Luker GD, et al (2007). CXCR7 (RDC1) promotes breast and lung tumor growth in vivo and is expressed on tumor-associated vasculature. *Proc Natl Acad Sci U S A* **104**, 15735–15740.

[31] Kryczek I, Lange A, Mottram P, Alvarez X, Cheng P, Hogan M, Moons L, Wei S, Zou L, and Machelon V, et al (2005). CXCL12 and vascular endothelial growth factor synergistically induce neoangiogenesis in human ovarian cancers. *Cancer Res* **65**, 465–472.

[32] Tabatabai G, Frank B, Mohle R, Weller M, and Wick W (2006). Irradiation and hypoxia promote homing of haematopoietic progenitor cells towards gliomas by TGF-beta-dependent HIF-1alpha–mediated induction of CXCL12. *Brain* **129**, 2426–2435.

[33] Schwenk MH (2010). Ferumoxytol: a new intravenous iron preparation for the treatment of iron deficiency anemia in patients with chronic kidney disease. *Pharmacotherapy* **30**, 70–79.